Electronic Supplementary Material (ESI) for Journal of Materials Chemistry B.

Supplementary Information

Schottky heterojunction CeO_2@MXene nanosheets with synergistic type I and type II PDT for anti-osteosarcoma

Bingxin Zheng, ‡[a] Ranran Zhang,‡[b] Fei Kuang, ‡[c] Tiankun Hui, ‡[b] Chenchen Fu,[b] Li Zhang, [d] Chuanli Zhou, [e] Meng Qiu[b] and Bin Yue*[a]*

a. Department of Orthopedic Oncology, The Affiliated Hospital of Qingdao University, Qingdao, Peoples Republic of China.

b. Key Laboratory of Marine Chemistry Theory and Technology (Ocean University of China), Ministry of Education, Qingdao 266100, China

c. Qingdao University, College of Life Sciences, 308 Ningxia Road, Qingdao, Shandong Province, China.

d. Department of Operating Room, The Affiliated Hospital of Qingdao University, Qingdao, People's Republic of China.

e. Department of Spinal Surgery, The Affiliated Hospital of Qingdao University, Qingdao, People's Republic of China.

‡ Contributed equally to this work.

* Corresponding author.

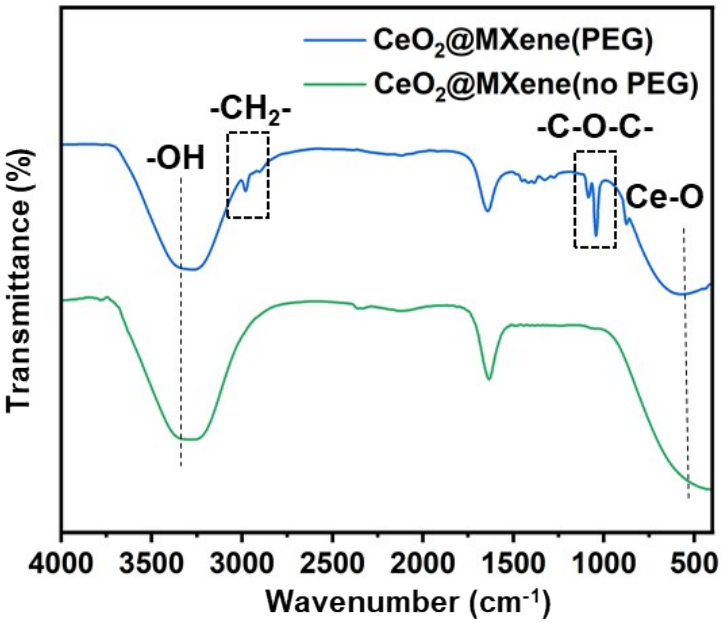

Fig. S1 The FT-IR spectra of CeO_2@MXene(PEG) and CeO_2@MXene(no PEG).

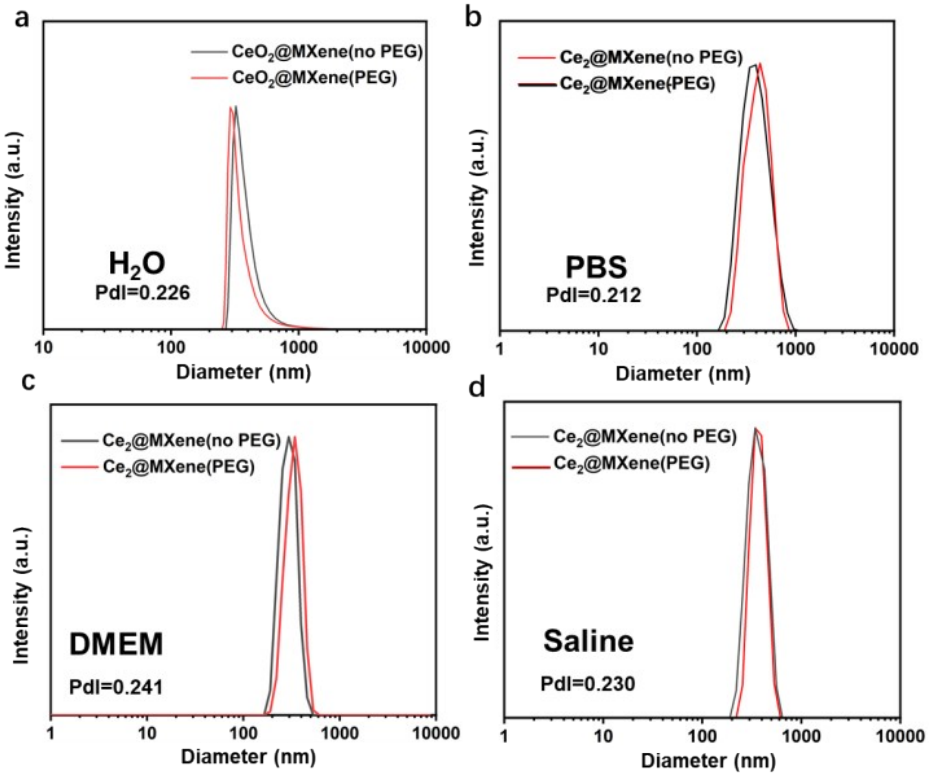

Fig. S2 The size distribution diagram of CeO_2@MXene(PEG) and CeO_2@MXene(no PEG) in different media.

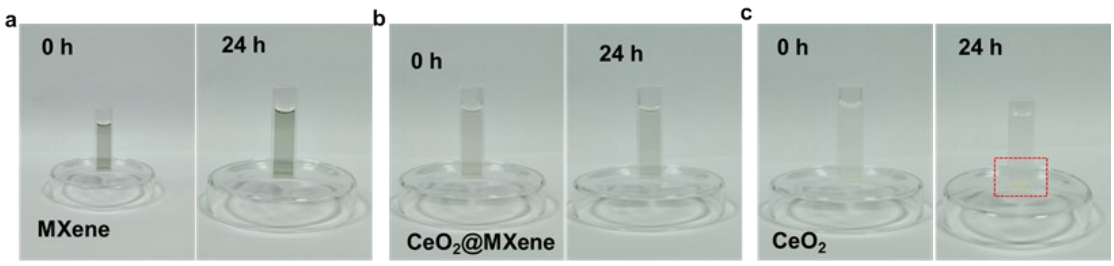

Fig. S3 Digital images of the materials dispersed in the solution.

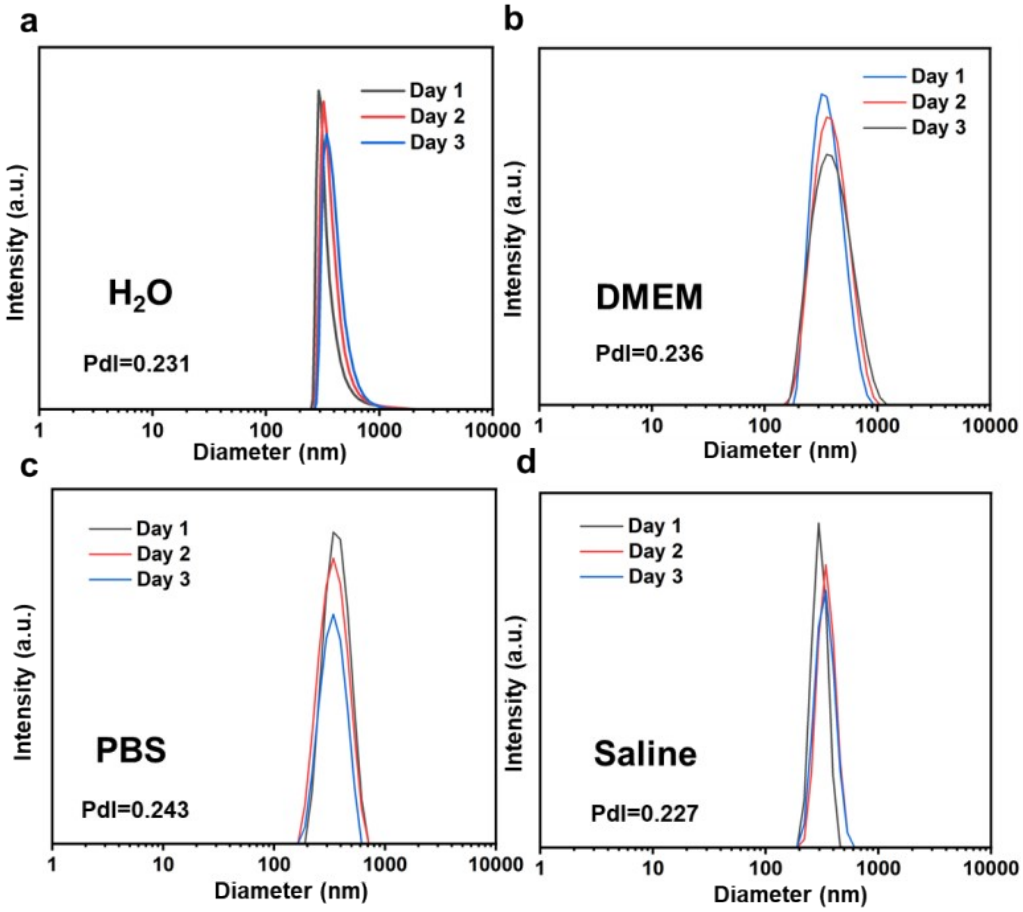

Fig. S4 The size distribution diagram of CeO_2@MXene(PEG) in different media within 3 days.

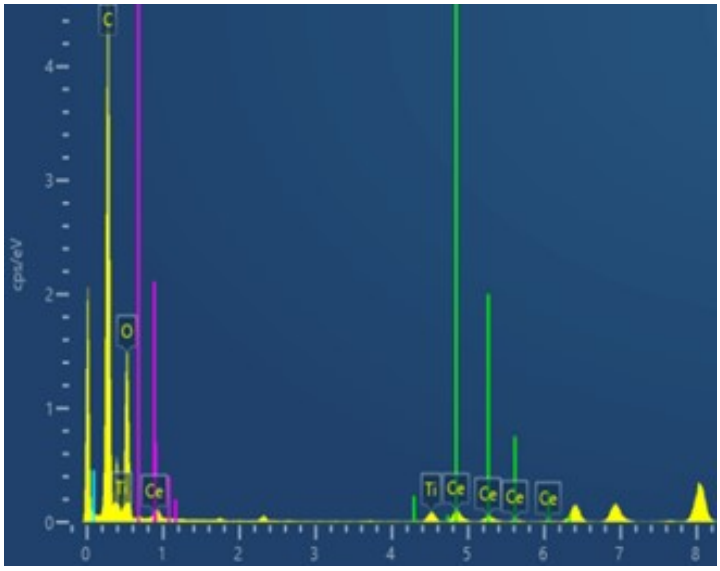

Fig. S5 Scanning spectrum of CeO_2@ MXene.

Elements	Mass percent	Atomic percent
C	9.31	22.10
O	26.89	47.91
Ti	43.41	25.84
Ce	20.38	4.15

Fig. S6 Contents of elements in CeO_2@MXene.

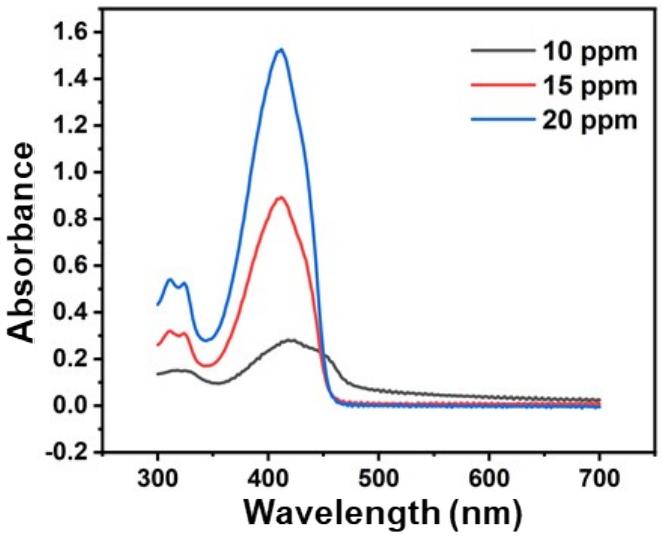

Fig. S7 Absorption spectra of CeO_2@MXene at different concentrations.

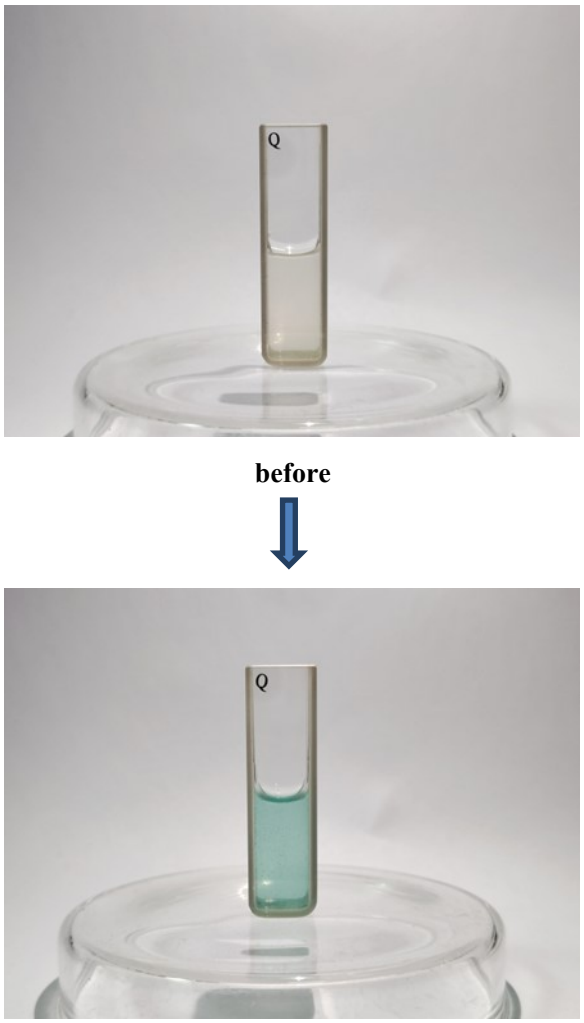

Fig. S8 Comparison of color changes before and after the color response of TMB and •OH.

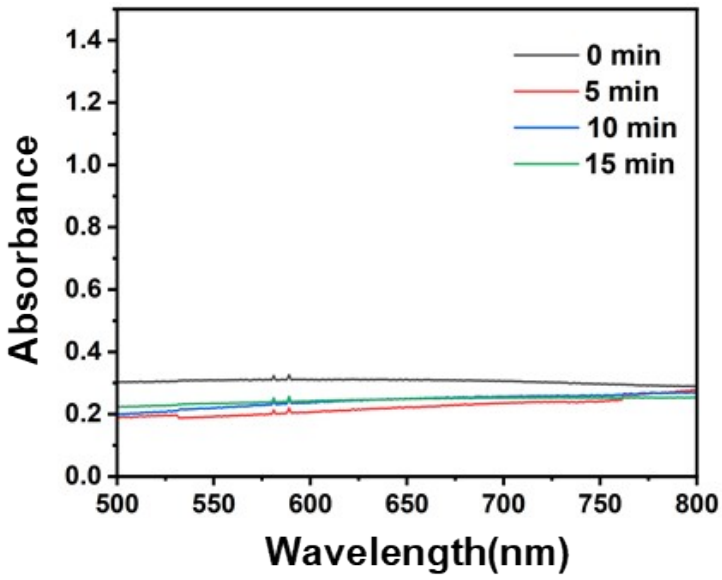

Fig. S9 Absorption spectra of TMB under different NIR irradiation time.

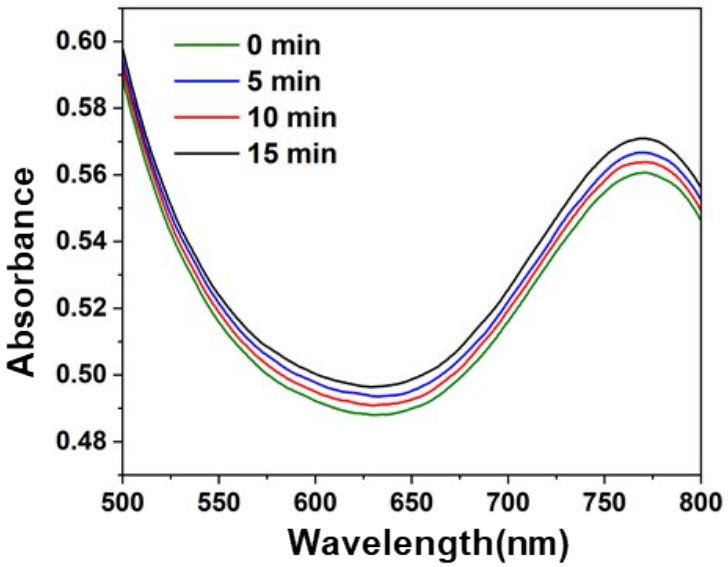

Fig. S10 Using TMB as probe, the formation of •OH generated by MXene was detected under different NIR irradiation time.

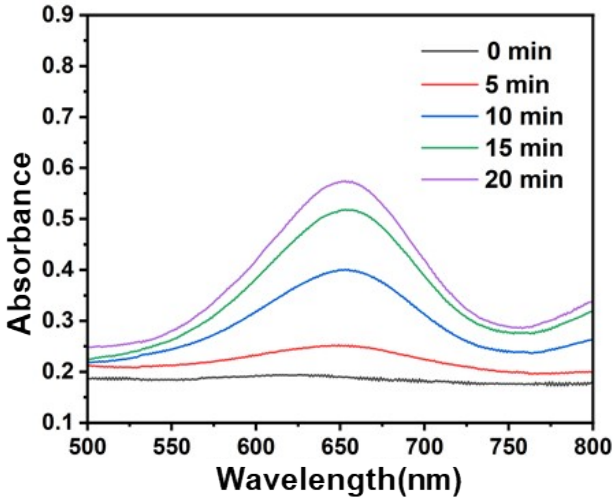

Fig. S11 Using TMB as probe, the formation of •OH generated by CeO_2 was detected under different NIR irradiation time.

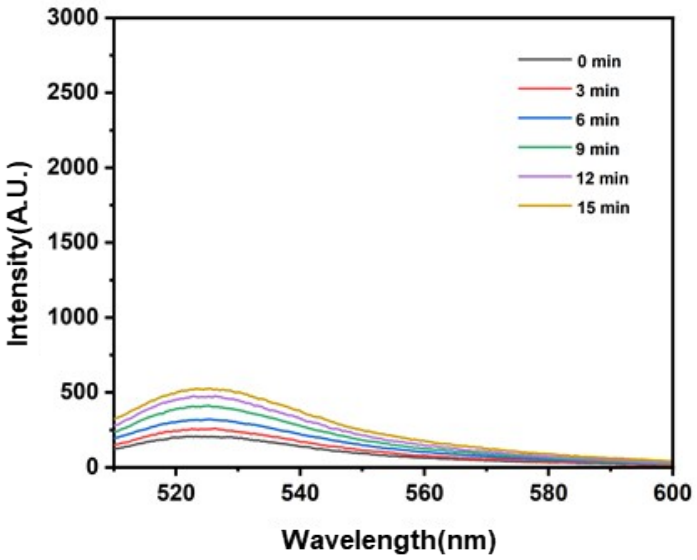

Fig. S12 Fluorescence spectra of DHR 123 fluorescent probe under different NIR irradiation time.

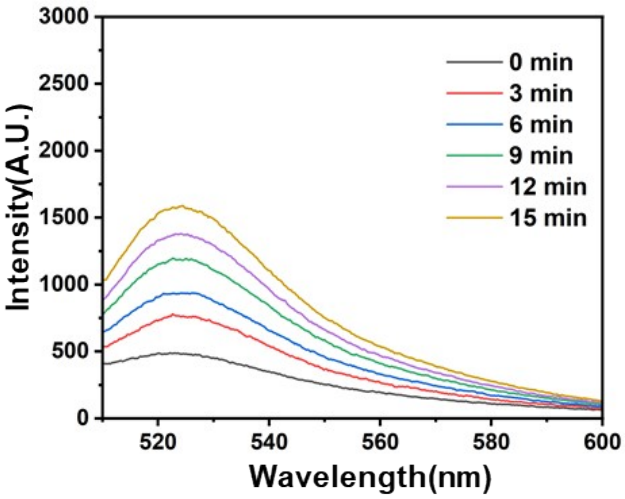

Fig. S13 DHR123 was used as a fluorescent probe to detect the formation of O_2^- generated by CeO_2 under different NIR irradiation time.

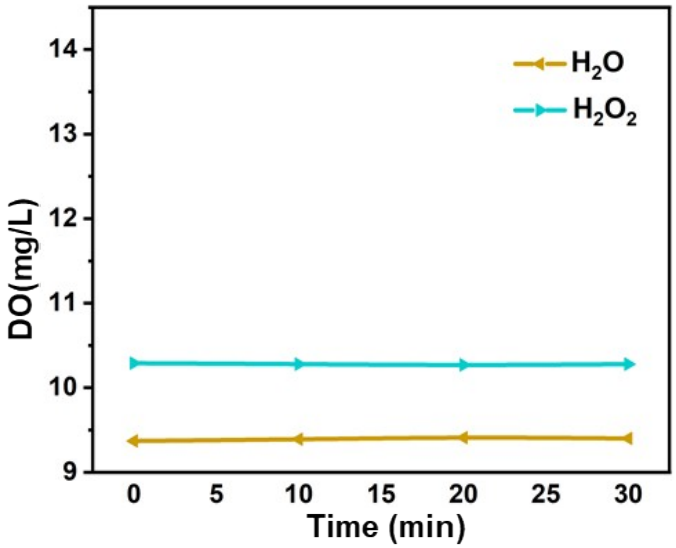

Fig. S14 Comparison of dissolved oxygen content in H_2O_2 and H_2O.

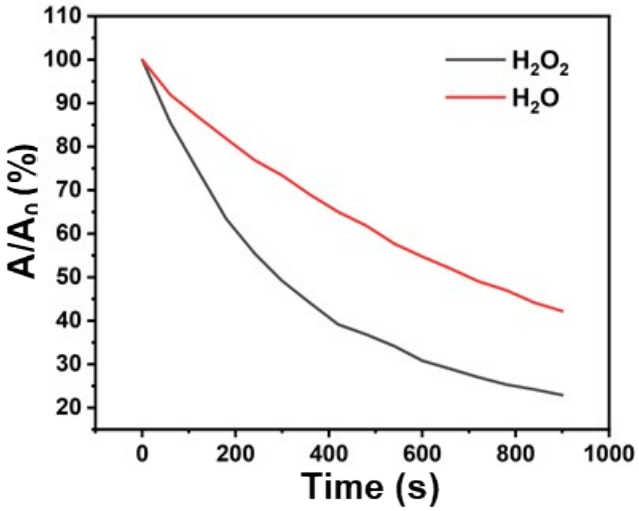

Fig. S15 Comparison of singlet oxygen production in two different liquid environments.

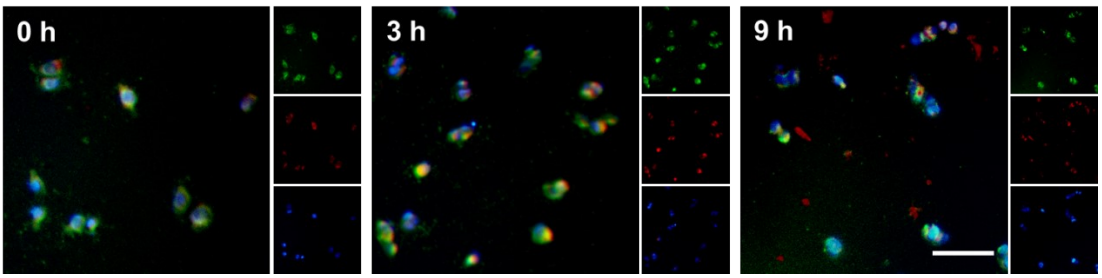

Fig. S16 The intracellular lysosome escape of MXene@CeO_2 in different time.